Pure & Appl. Chem., Vol. 70, No. 3, pp. 671–676, 1998.
Printed in Great Britain.

Multi-state thermal transitions of proteins— DNA-binding domain of the *c*-Myb oncoprotein

Hatsuho Uedaira[a], Hisayuki Morii[b], Kazuhiro Ogata[a], Shunsuke Ishii[a], and Akinori Sarai[a]

[a]*Tsukuba Life Science Center, The Institute of Physical & Chemical Research (RIKEN), Tsukuba, 305 Japan*
[b]*National Institute of Bioscience and Human-Technology (NIBH), Tsukuba, 305 Japan*

Abstract: The DNA binding domain of *c*-Myb protein, a regulator of the transcription, consists of three homologous tandem repeats (R1, R2 and R3) with 51-52 amino acid residues. Previously, we found that the thermal transition of the binding domain (R1R2R3) is three-state transition and that the intermediate state is related to the lower stability of R2 than the other two. In order to clarify the thermodynamic characteristics of the most unstable R2, we synthesized two mutants of R2, R2(V103I) and R2(V103L), and examined their thermodynamic properties by circular dichroism and differential scanning calorimetry. The thermal transition temperature (T_d) and enthalpy change (ΔH) obtained by CD for R2(V103I) and R2(V103L) were 47.1 and 62.6 °C, and 144 and 166 kJ mol^{-1}, respectively. The corresponding values by DSC were 47.5 and 62.8 °C, and 140.1 and 173.4 kJ mol^{-1}, respectively. Especially, the values of T_d and ΔH for R2(V103L) by CD (DSC) are significantly higher than those for R2, which are 43.7 (43.8) °C and 125.4 (133.6) kJ mol^{-1}. The larger stabilizing effect by the substitution was found for Leu mutant. The results suggest that not only the cavity effect but also the contributions of conformational change in native and denatured states, and of the interactions of the side chains with water should be taken into account.

INTRODUCTION

Many proteins which have multi-domain structure with different thermal stability show multi-state thermal transitions (1). While, the proteins which are composed of two merged interacting structural domains with the comparable thermal stability, show two state transition. Even in this case, if one of the domains are made relatively less stable by mutation or variation of solution condition, it results in non-two-state transition of the proteins. For example, Carra et al. investigated the effect of destabilizing mutations of the N-terminal region of T4 lysozyme on the unfolding behavior (2). They demonstrated that a three-state unfolding model including a discrete intermediate was necessary to describe the melting of the mutant proteins, whereas the pseudo-wild-type reference protein thermally unfolded in an essentially two-state manner.

Accurate thermodynamic measurements of intermediate states in the protein folding/unfolding process provide the knowledge to elucidate the energetics and mechanisms of native protein structure. The DNA binding domain of *c*-Myb protein, a transcriptional regulatory factor, consists of three homologous tandem repeats (R1, R2 and R3) with 51-52 amino acid residues (3). The homologies between R1 and R2, R2 and R3, and R3 and R1 are 46%, 31%, and 33%, respectively. The solution structures of the three repeats have been determined by NMR analysis (4, 5). Each repeat has conformation similar to helix-turn-helix motif with three well-defined helices. Three conservative tryptophans in each repeat participate in forming a hydrophobic core, which definitely characterizes the structure of the repeat. Comparison of the three repeat structures indicated that there existed a cavity in the hydrophobic core of R2. Val is located at the position 103 in the first helix of R2, whereas the corresponding amino acids in R1 and R3 are more bulky Leu 51 and Ile155, respectively (5). The presence of the cavity in R2 was found to cause conformational flexibility of R2 and play an important role in binding and recognition of DNA (5, 6). The cavity also decreases the conformational stability of R2 compared with R1 and R3, which gives rise to the three-state thermal transition of R1R2R3 (7) and R2R3 (6). The mutant of R2R3 in which Val 103 in R2 is replaced to Leu showed higher thermal stability than wild-type R2R3 (6). Both wild type and the mutant of R2R3 were

found to behave as three-state transition, which indicated that there is a difference in thermal stability not only between R2 and R3 but also R2(V103L) and R3. As R3 was not changed in both R2R3 and R2(V103L)R3, one of the cooperative transition components with T_d near that of isolated R3 was attributed to the transition of R3 in both wild type and the mutant of R2R3. Consequently, the value of T_d for R2 unit (47 °C) in the wild-type R2R3 was found to shift drastically to 66 °C in mutated R2(V103L)R3 (6). From these results the following questions arise: whether (i) R2 by itself, when Val103 is substituted to Leu, is stabilized as much as 19 °C or not; (ii) the destabilization of R2 is caused only by the cavity in the core region or not; (iii) the local conformation and the cavity of R2 are affected by the substitution to more bulky or smaller amino acid side chains or not.

In order to clarify these thermodynamic characteristics of R2, we started to investigate several mutants of R2. Here we report the results on the thermal transition behavior of R2 and its two mutants, R2(V103L) and R2(V103I), measured by circular dichroism (CD) and differential scanning calorimetry (DSC). The results are discussed on the basis of cavity and hydration effects and also compared with those of R2R3 and R1R2R3.

EXPERIMENTAL

Preparation of proteins and solutions

R2 and its two mutants, R2(V103L) and R2(V103I), were chemically synthesized by usual solid phase method. The peptides were purified by reversed-phase high performance liquid chromatography (HPLC) using water-acetonitrile gradient elution. They were lyophilized for storage and dissolved in a desired buffer solution just before use.

The purified samples were dissolved in 50 mM potassium phosphate buffer solution (pH 7.5) containing 50 mM KCl and 10 mM dithiothreitol (DTT), and dialyzed against the buffer without DTT. All of the buffer solutions were bubbled with nitrogen gas at least two hours before use. The outer buffer solution was also continuously bubbled with nitrogen gas during the dialysis.

DSC and CD measurements

In order to avoid undesirable reaction with Cys130 in R2, 10 mM of DTT was added to the solutions for CD measurements. Degassing of the solutions were made before the DSC measurements and the solution pressure was recovered to 1 atm by filling with Argon. CD spectra at 10 °C and their temperature dependency were measured with Jasco J600 spectropolarimeter. Measurements were made using a optical cells with a 0.02-cm path length. Thermal transition was monitored by the change of CD at 222 nm. Temperature dependency of heat capacity was measured with MicroCal MCS differential scanning calorimeter. Heating rate of CD and DSC was 0.75 K min^{-1}. Concentration of proteins for CD and DSC measurements were 60-120 μM and 120-230 μM, respectively.

RESULTS AND DISCUSSION

The relation between the thermodynamic properties of individual repeat and R1R2R3

First, we examined the additivity of CD spectrum for R1R2R3 from its composition by the calculation based on the additivity of R1, R2 and R3, by taking into account of their amino acid residue composition. The CD spectrum of R1R2R3 coincides completely with the calculated curve at 10 °C (Fig. 1A), but the calculated curve at 85 °C showed some discrepancy (data are not shown). The results of CD at 10 °C is in agreement with the results of NMR, that is, in the native state the secondary and tertiary structures of the isolated individual repeat fragments are conserved in both R1R2R3 and R2R3 (5). Ogata et al. further demonstrated that each repeat in solution forms an entirely independent structural unit with successive units connected by loops, and that the relative orientations of the three repeats are not fixed. Consequently, we can discuss thermodynamic data on the bases that the native structure of each repeat is the same as that in R1R2R3 and/or R2R3.

We analyzed the temperature dependence of molar ellipticity at 222 nm, for R1, R2 and R3 (7) on the assumption of two-state transition. The mole fractions of denatured forms of R1, R2, R3, and R1R2R3 are shown in Fig. 1B, together with the calculated curve for R1R2R3 from the constituent three repeats. The thermal transition temperature (T_d), at which the free energy change of thermal transition ($\Delta G(T)$) is equal to zero, and enthalpy changes (ΔH) for R1, R2 and R3 are 60.2, 43.7, and 56.1 °C and 175.6, 125.4, and 180.6 kJ mol^{-1}, respectively. As described before (6), the main reason for the smallest values of T_d and ΔH for R2 has been attributed to the cavity in the hydrophobic core.

The calculated mole fraction of the denatured form for R1R2R3 did not coincide with the experimental curve for R1R2R3. Interactions between the repeats might affect the unfolding process of R1R2R3.

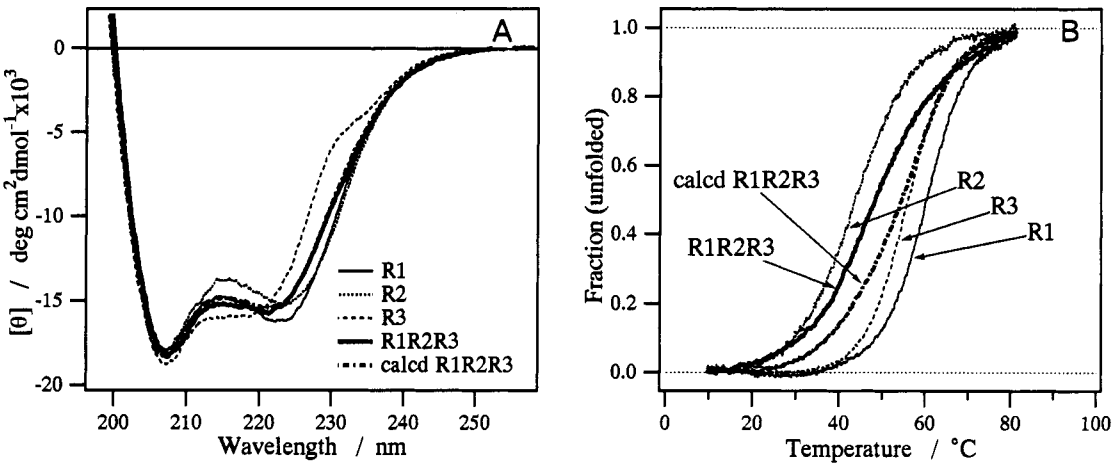

Fig. 1 CD spectra at 10°C (A) and the temperature dependence of the fraction of unfolded states calculated from molar ellipticity at 222 nm (B) for R1, R2, R3, and R1R2R3. The calculated curves of R1R2R3 based on the additivity of the components were superimposed.

Analysis of the thermal transition of R2R3 and its mutant

The thermal transition curves for R2R3 and its mutant at the position of Val103, R2(V103L)R3, showed three-state transition, as reported before (6). We analyzed the DSC data (6) by the double deconvolution method (8), and calculated heat capacity curves were further adjusted by a nonlinear least-squares fitting method (9), using the SALS program (10). As shown in Fig. 2A, the calculated curves fitted fairly well to the experimental data (The RMSD for R2R3 and R2(V103L)R3 are 0.43 and 0.63 μW, respectively).

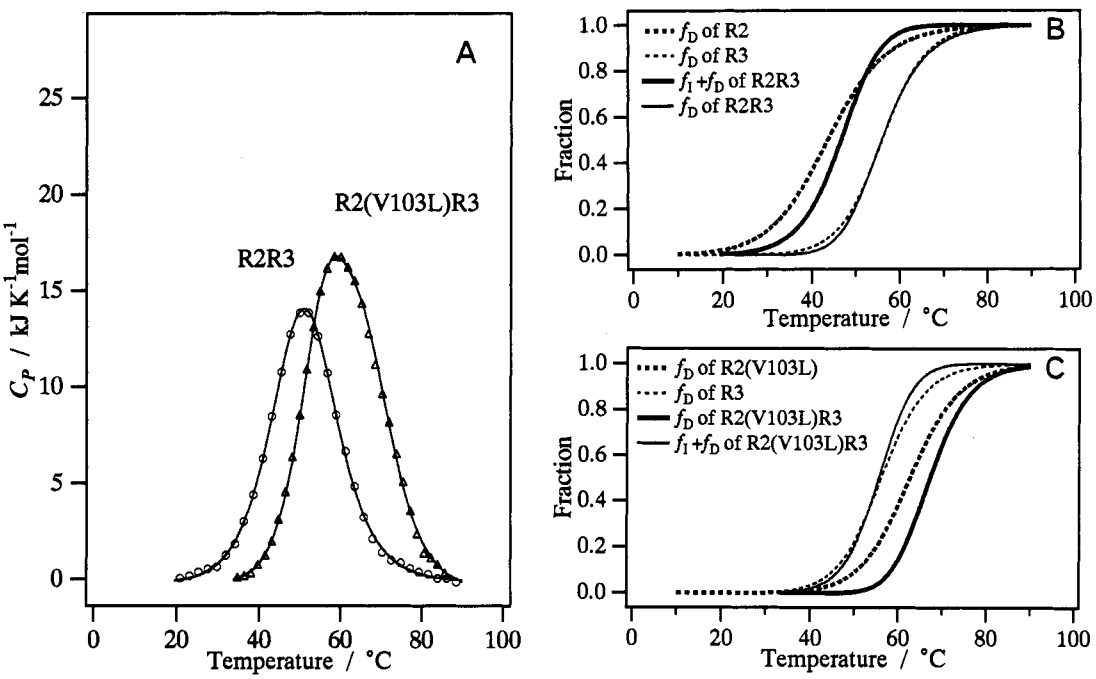

Fig. 2 DSC curves for R2R3 (circles) and R2(V103)R3 (triangles), and calculated fit curves (solid lines) (A); fraction of thermodynamic states for R2R3 (B) and R2(V103L)R3 (C). Thick or thin solid lines denote $f_I + f_D$ or f_D by DSC. Thick and thin dotted lines denote f_D for R2 or R2(V103L), and for R3 by CD, respectively.

The values of T_d and ΔH for the native to intermediate, and intermediate to denatured states for R2R3 are, 47.9, 54.7 °C and 153.3 and 154.0 kJ mol^{-1}, respectively. Similarly, those for the R2(V103L)R3 are, 55.8, 66.7 °C and 208.9 and 196.4 kJ mol^{-1}, respectively. Mole fractions of intermediate and denatured states for R2R3 and R2(V103L)R3 were calculated from fitted parameters and are shown in Fig. 2B and 2C, together with the experimental and calculated heat capacity curves (Fig. 2A). The agreement between the thin solid and the thin dotted lines indicates that the thermal transition with higher T_d in R2R3 and the one with lower T_d in R2(V103L)R3 correspond to R3 unit. Though the heat capacity difference between native and denatured states may exist, it was assumed to be zero because of the difficulty in precise determination from the base lines of the heat capacity data (6).

The secondary structure and thermal transition behaviors of R2 and its mutants

The values of T_d from the intermediate to denatured state in R2R3, which is close to T_d of the transition between the native and intermediate states, corresponds to the denaturation of R3 as described before (6). The other cooperative unit in R2R3 and R2(V103L)R3 should be the transition of R2. Consequently, T_d of R2 part increased from 47.9 to 66.7 °C by the mutation of Val103 to Leu. To confirm this stabilization experimentally, and for the comparison, we synthesized two mutants, R2(V103L) and R2(V103I), and measured their thermal transition. Far UV CD spectra for wild-type R2, R2(V103I) and R2(V103L) at 10 °C are shown in Fig. 3A. The shape and depth of the three curves around 220 nm coincide fairly well. A slight difference at around 230 nm seems to reflect different condition of Trp side chains. These results coincide with the analysis of R2R3 and R2(V103L)R3 by NMR (6), which shows that the effects of the replacement are only local and the tertiary structure of backbones is almost unaltered.

Temperature dependence of molar ellipticity at 222 nm is shown in Fig. 3B with the calculated curves on the assumption of two-state transition. The calculated curves did not show much difference when the values of ΔC_P were assumed to be 0-5 kJ K^{-1}mol^{-1}. Consequently, for the first approximation, we fixed the value of ΔC_P at zero. The values of T_d and enthalpy of the transition at T_d for R2, R2(V103I) and R2(V103L) are 43.7, 47.1 and 62.6 °C, and 125, 144 and 166 kJ mol^{-1}, respectively.

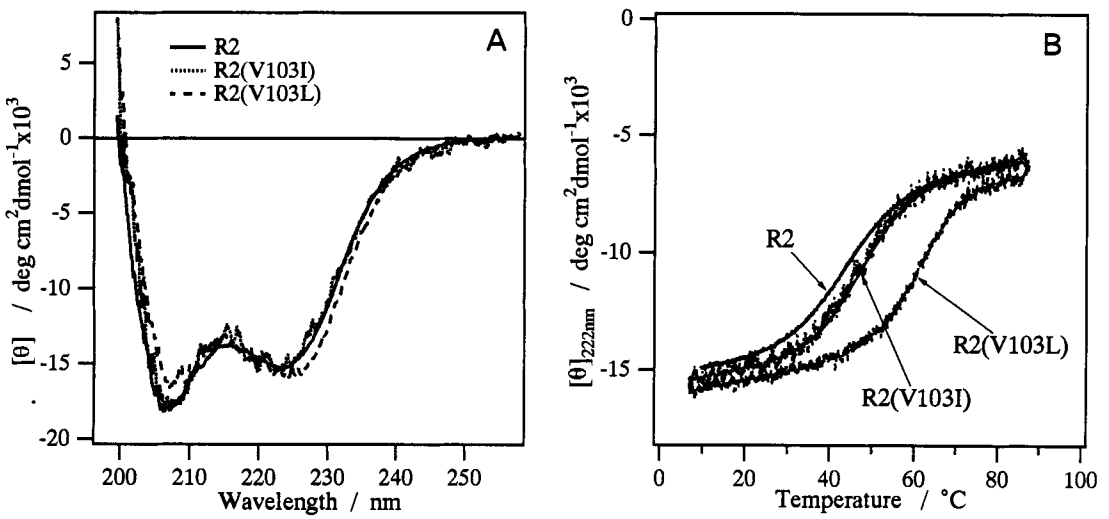

Fig. 3 Far UV CD spectra of R2 (solid), R2(V103I) (dotted) and R2(V103L) (dashed) (A); the temperature dependence of molar ellipticity at 222 nm for wild-type R2 and two mutants (B).

The DSC curves for R2, R2(V103I), and R2(V103L) are summarized in Fig. 4. The calculated values of T_d and ΔH for R2, R2(V103I) and R2(V103L) on the assumption of two-state transition are 43.8, 47.5, and 62.8 °C, and 133.6, 140.1 and 173.4 kJ mol^{-1}, respectively. The values obtained for R2's by CD and DSC agreed fairly well. The mutant, R2(V103L), has an extremely high thermal stability compared with the others. By the deconvolution of the thermal transitions of R2R3 and R2(V103L)R3, the values of T_d and ΔH for R2 and R2(V103L) units are calculated to be 47.9 and 66.7 °C, and 153.3 and 196.4 kJ mol^{-1}, respectively. The corresponding values for isolated R2 and R2(V103L) are 43.8 and 62.8 °C, and 133.6 and 173.4 kJ mol^{-1}, respectively. These values for isolated R2's are about 4 °C lower and 20 kJ mol^{-1} smaller than the above values for the corresponding units in R2R3's. By NMR analysis R2 and R3 are found to be independent repeats, however, from the view point of thermodynamics, there seems to exist a small stabilizing joint effect.

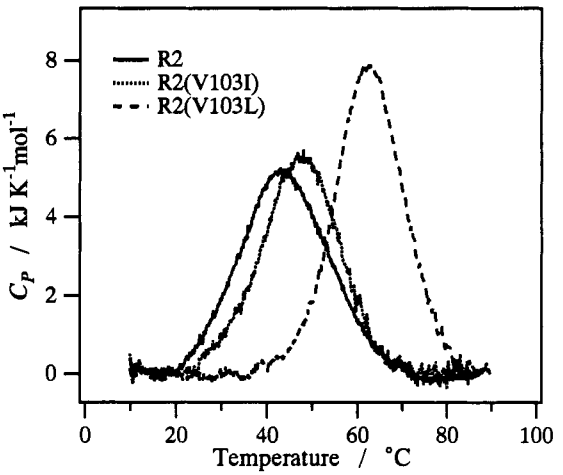

Fig. 4 Excess heat capacity curves for R2 and its mutants. The solid, dotted, and dashed lines denote R2, R2(V103I), and R2(V103L), respectively.

The factors which affect the thermodynamics of the transition of R2 and its mutants

As mentioned above, the substitution from Val103 to Ile or Leu in R2 was found to remarkably stabilize the protein. The difference in free energy of the transition at T_d of R2 for R2(V103I) and R2(V103L) are calculated to be 1.53 and 9.37 kJ mol^{-1}, respectively. The lower thermal stability of R2 than those of R1 and R3 has been attributed mainly to the existence of the cavity in R2 (6). As a similar case, the decrease in the stability of four-helix bundle protein, repressor of primer (ROP), was observed by the cavity creating mutation, L41V (10). The substitution of Leu to Val decreased the value of T_d (71 °C for wild-type ROP) by 6-7 °C, and $\Delta\Delta G$ was -5.3 kJ (monomer mol)$^{-1}$ at 25 °C.

Generally, the effect of aliphatic amino acid substitution at cavity on the change in unfolding free energies can be explained by three contributions. One is the cavity effect and the second is the conformational change in both native and unfolded states. The third one is the effect by the change in interaction with solvent water.

The van der Waals volumes of the amino acid side chains for Leu and Ile are the same. Since the difference in the van der Waals volume of the Leu and Val are 14.03 Å^3 (11), the corresponding free energy term that increases with increasing the size of cavity is 1.41-1.94 kJ mol^{-1} (12), which is about the same for Ile substituent and one fifth for Leu substituent. The NMR structural analysis revealed that the main chain structure did not change by the substitution from Val to Leu (6), however, the structure of Ile mutant has not yet been analyzed.

The change in the thermal stability by the substitution of amino acid from Ile to Leu in the cavity region of R3 has been found (13). The amino acid residues, Ile155, Ile181 and His184, forms the hydrophobic core of R3, which corresponds to the hydrophobic core formed with Val103 Cys130 and Arg133 in R2 (5). The thermal transition temperature of I155L mutant of R3 was observed to be 59.6 °C, which is higher than that of wild-type R3 by 3.7 °C (13). The backbone structure of I155L is very similar to the wild type, however, both the indole ring of Trp147 and the imidazole ring of His184 was found to tilt by about 30 degree from those of the wild type. ^{1}H-^{2}H exchange experiments showed that the protection factors of I155L mutant were comparable to those of wild type. These facts mean that the native backbone structures of R3 and the mutant, I155L, are almost the same, but the precise structure including side chain conformation is not strictly the same. Furukawa et al. calculated the change in side-chain conformational entropy for the Leu substitution of Ile155 to be 27.21 J K^{-1}(residue mol)$^{-1}$ at 300 K (13). The increased side chain entropy affects to stabilize the native conformation. Increasing a cavity by amino acid substitution will result in relaxation of the protein structure and also cause the change in flexibility. The free energies associated with all relaxation process were defined as ΔG^{relax} by Honig and Yang (14). It remains possible that some local change, which is related to ΔG^{relax}, might occur by the above amino acid substitution of R2.

The energetics of protein folding/unfolding involve contributions from the solvent as well as the configuration. Concerning the enthalpy change, the calculated values for α-helix unfolding for Val, Ile and Leu are, 3.42, 4.61, and 4.54 kJ mol^{-1} at 25 °C (15). Regarding the entropy, the increase in backbone entropy upon unfolding is also increased by 5.14 J K^{-1}mol^{-1} (16), when the β-branching amino acid residues, Val and Ile, are substituted to γ-branching Leu. Contrary to the experimental results, this effect causes the destabilization of Leu mutant compared with Val and Ile.

The calculated total configurational entropy change for the exposed side chain in α-helix to the unfolded state are 5.44, 2.80 and 1.05 J K^{-1}mol^{-1} for Val, Ile and Leu, respectively (15), which correspond to the

contribution to free energy of unfolding, -1.62, -0.83, and -0.31 kJ mol^{-1} at 25 °C. Consequently, the order of the entropic destabilizing effects is Val>Ile>Leu. This effect also can partly explain the stronger stabilization by Leu than Ile.

The solvent contribution can be effectively parameterized as a function of the change in exposed polar and apolar areas. The hydration of the hydrophobic alkyl side chains can be calculated on the bases of the transfer of small molecules from vacuum to water (17). As the transfer free energy of amino acid side chains from vapor to water for Val, Ile, and Leu are 8.33, 9.00, and 9.54 kJ mol^{-1}, respectively (18), this contribution stabilizes the protein native state in the order of Leu>Ile>Val.

In addition, the dynamic properties of the hydration of the hydrophobic amino acids were studied by NMR (11). The dynamic hydration number (n_{DHN}) were obtained from the measurements of the spin-lattice relaxation times, T_1, of $H_2{}^{17}O$ for the amino acid solutions at 25 °C. The values of n_{DHN} are proportional to the change in entropy decrease of hydration (19) and the obtained values for Val, Ile and Leu are 20.1, 25.6 and 26.6, respectively (11). The experimental values of $\Delta\Delta G$ for Ile and Leu substitutions of Val in R2 are affected by these various contributions.

The experimental thermodynamic results of the mutants of R2 suggest that the contributions of conformational change in native and denatured states, and of the interactions of the side chains with water, as well as the cavity effect, should be taken into account. R2 has a definite hydrophobic core inside the molecule in spite of its small molecular weight, and this core with a cavity has an important roll in recognition of DNA by *c*-Myb. The studies of R2 with a variety of hydrophobic amino acid substitutions are ongoing, and the results would elucidate experimentally the relationship among the structure, energetics, and functions of *c*-Myb DNA-binding domain more clearly.

ACKNOWLEDGMENTS

The authors are grateful to Dr. Hidetoshi Kono (RIKEN) for the valuable discussion and the kind help in computation.

REFERENCES

1. P. L. Privalov, *Adv. Protein Chem.*, **35**, 1 (1982).
2. J. H. Carra, E. C. Murphy and P. L. Privalov, *Biophys. J.*, **71**, 1994 (1996).
3. H. Sakura, C. Kanei-Ishii, T. Nagase, H. Nakagoshi, T. J. Gonda and S. Ishii, *Proc. Natl. Acad. Sci. U.S.A.*, **86**, 5758 (1989).
4. K. Ogata, H. Hojo, S. Aimoto, T. Nakai, H. Nakamura, A. Sarai, S. Ishii and T. Nishimura, *Proc. Natl. Acad. Sci., U.S.A.*, **89**, 6428 (1992).
5. K. Ogata, S. Morikawa, H. Nakamura, H. Hojo, S. Yoshimura, R. Zhang, S. Aimoto, Y. Ametani, Z. Hirata, A. Sarai, S. Ishii and Y. Nishimura, *Nature Struct. Biol.*, **2**, 309 (1995).
6. K. Ogata, C. Kanei-Ishii, M. Sasaki, H. Hatanaka, A. Nagadoi, M. Enari, H. Nakamura, Y. Nishimura, S. Ishii and A. Sarai, *Nature Struct. Biol.*, **3**, 178 (1996).
7. A. Sarai, H. Uedaira, H. Morii, T. Yasukawa, K. Ogata, Y. Nakamura and S. Ishii, *Biochemistry*, **32**, 7759 (1993).
8. S. Kidokoro and A. Wada, *Biopolymers*, **26**, 213 (1987).
9. S. Kidokoro, H. Uedaira and A. Wada, *Biopolymers*, **27**, 271 (1988).
10. C. Steif, H.-J. Hinz and G. Cesareni, *Proteins*, **23**, 83 (1995).
11. M. Ishimura and Hi. Uedaira, *Bull. Chem. Soc. Jpn.*, **63**, 1 (1990).
12. A. E. Eriksson, W. A. Baase, X. -J. Zhang, D. W. Heinz, M. Blaber, E. P. Baldwin and B. W. Matthews, *Science*, **255**, 178 (1992).
13. K. Furukawa, M. Oda and H. Nakamura, *Prod. Natl. Acad. Sci. U.S.A.*, **93**, 13583 (1996).
14. B. Honig and A.-S. Yang, *Adv. Protein Chem.*, **46**, 27 (1995).
15. K. H. Lee, D. Xie, E. Freire and L. M. Amzel, *Proteins*, **20**, 68 (1994).
16. J. A. D'Aquino, J. Gomez, V. J. Hilser, K. H. Lee, L. M. Amzel and E. Freire, *Proteins*, **25**, 143 (1996).
17. G. I. Makhatadze and P. L. Privalov, *Adv. Protein Chem.*, **47**, 307 (1995).
18. A. Radizka and R. Wolfenden, *Biochemistry*, **27**, 1664 (1988).
19. S. Okouchi, T. Moto, Y. Ishihara, H. Numajiri and Hi. Uedaira, *J. Chem. Soc. Faraday Trans.*, **92**, 1853 (1996).